THE JOURNAL OF PHYSICAL CHEMISTRY C

Article

Cite This: J. Phys. Chem. C 2019, 123, 27369−27374

pubs.acs.org/JPCC

Impacts of Ethanol and Water Adsorptions on Thermal Conductivity of ZIF-8

Wei Wei,[†,‡] Jun Huang,[§] Wei Li,[‡] Haiyan Peng,*[,†] and Song Li*[,‡]

[†]Key Lab for Material Chemistry of Energy Conversion and Storage, Ministry of Education, School of Chemistry and Chemical Engineering and [‡]State Key Laboratory of Coal Combustion, School of Energy and Power Engineering, Huazhong University of Science and Technology, Wuhan 430074, Hubei, China

[§]Key Laboratory for Thermal Science and Power Engineering of Ministry of Education, Department of Engineering Mechanics, Tsinghua University, Beijing 100084, China

Supporting Information

ABSTRACT: Metal−organic frameworks are promising nanoporous materials for adsorption heat pumps (AHPs) using water and alcohols as working fluids due to their ultrahigh surface area. The heat transfer in porous crystals containing adsorbed gases is vital for their performance in adsorbed natural gas storage or AHPs. However, limited attention has been paid to their thermal properties. In this study, equilibrium molecular dynamics simulations were performed to investigate the impacts of ethanol/water adsorption on the thermal conductivity of zeolitic imidazolate framework-8 (ZIF-8). The results demonstrated that the thermal conductivity of ZIF-8 increased from 0.165 to 0.319 W m^{-1} K^{-1} with the increased number of adsorbed ethanol molecules. On the contrary, the thermal conductivity of ZIF-8 upon water adsorption is approximately 0.190 W m^{-1} K^{-1}, which is not significantly affected by the number of adsorbed water molecules. Such a different tendency may be ascribed to the different interaction strengths between ZIF-8 and gas molecules. In addition, the larger overlap energy in the vibrational density of state of ZIF-8/ethanol than that of ZIF-8/water also correlates with the higher thermal conductivity of the ZIF-8/ethanol system. This work provides molecular insights into the effects of ethanol/water adsorption on the thermal conductivity of ZIF-8, which may inspire further exploration of novel techniques to improve the heat transfer performance of practical applications.

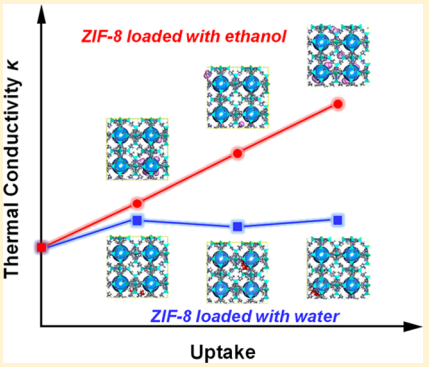

1. INTRODUCTION

Metal−organic frameworks (MOFs) consisting of metal clusters and organic linkers are a unique class of hybrid porous materials that has been used in gas storage,[1,2] gas separation,[3] sensing,[4] catalysis,[5] and water harvesting from air[6] due to their large surface area and high porosity.[7] MOFs are also recognized as potential adsorbents for adsorbed natural gas storage[8−10] and adsorption heat pumps (AHPs) using water and alcohols as working fluids.[11] Heat transfer has been involved in gas adsorption and desorption processes of these applications. Thus, the thermophysical properties of MOFs are crucial in determining how quickly storage vessels can be filled[10] or emptied.

The thermal conductivities of MOFs with adsorbed hydrogen and methane have been investigated by molecular simulation in recent studies. Han et al.[12] investigated heat transfer properties of MOF-5 with adsorbed hydrogen and deuterium by molecular dynamics (MD) simulations. It was revealed that the thermal conductivity of MOF-5 was slightly increased upon hydrogen adsorption, which was ascribed to additional channels for heat transfer from nodes to linkers provided by gas adsorption. Babaei et al.[13] demonstrated the slightly decreased thermal conductivity with methane uptake, which was mainly the result of phonon scattering in the crystals due to interactions with gas molecules. In addition, MD simulations also revealed that methane imposed insignificant impacts on the thermal conductivity of idealized metal−organic frameworks.[14]

From the above studies, the adsorption of either hydrogen or methane gas that exhibits weak interaction with MOFs does not make remarkable contribution to the thermal conductivity of MOFs. However, the thermal conductivity of MOFs upon polar gas adsorption such as water or alcohols has been rarely reported. Besides, from the perspective of experimental measurements, heat transfer performance of MOFs has been scarcely measured. Until now, thermal conductivities of single-crystal zeolitic imidazolate framework-8 (ZIF-8),[15] MOF-1,[16] and MOF-5[17] at room temperature have been measured to be 0.33, 1.3, and 0.32 W m^{-1} K^{-1}, respectively, which agrees with the predicted results by MD simulations (0.31 W m^{-1} K^{-1} for MOF-5[18] and 0.165 W m^{-1} K^{-1} for ZIF-8[19]). The remarkably enhanced thermal conductivities of Cu-BTC, UiO-66, and UiO-67 upon water vapor adsorption have been observed in experimental measurements,[20] implicating the significant

Received: August 27, 2019
Revised: October 23, 2019
Published: October 23, 2019

DOI: 10.1021/acs.jpcc.9b08187
J. Phys. Chem. C 2019, 123, 27369−27374

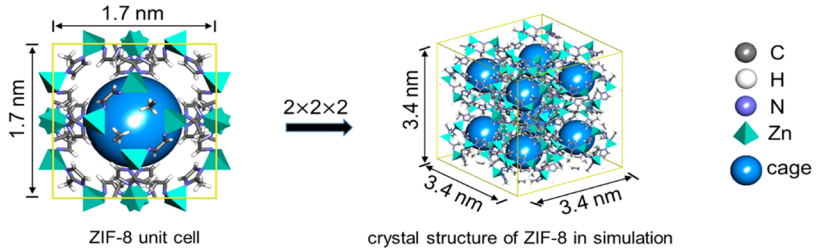

Figure 1. ZIF-8 unit cell and 2 × 2 × 2 supercell structure. Zn (cyan polyhedron), N (medium slate blue sphere), C (gray sphere), and H (white sphere). The large blue spheres represent the largest cavities that would fit in the pore of the framework.

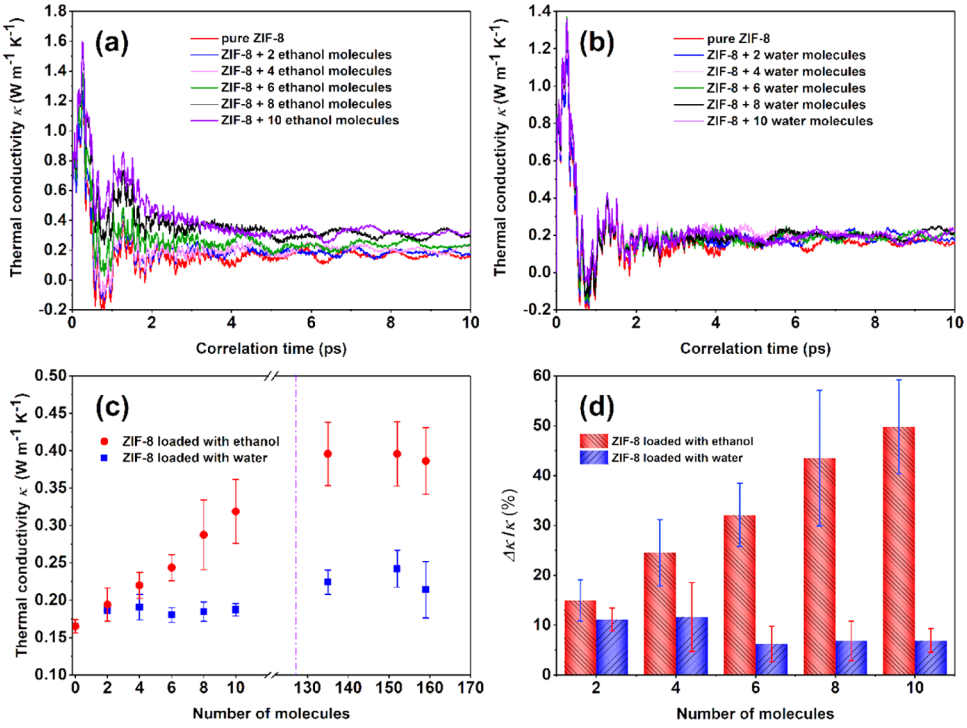

Figure 2. Thermal conductivity of ZIF with adsorbed (a) ethanol/(b) water at 300 K as a function of correlation time in systems. (c) Thermal conductivity of ZIF-8 as a function of adsorbed number of ethanol/water molecules. (d) Increment of thermal conductivity ($\Delta\kappa$) relative to the total thermal conductivity (κ).

influence of water adsorption on the thermal conductivity of MOFs. However, the impacts of adsorption of different polar gases on the thermal conductivity of MOFs remains to be explored.

In this study, both ethanol and water were used as adsorbates. ZIF-8 was chosen as a representative MOF due to its high chemical, mechanical, and thermal stabilities. Besides, ZIF-8 is known to exhibit a high ethanol adsorption capacity and low water uptake due to its high hydrophobicity.[21−23] Therefore, ZIF-8 can be a good example of typical MOF to demonstrate the influences of the polar gases that exhibit different affinities toward ZIF-8 on its thermal conductivity. Therefore, the effects of ethanol and water adsorption on the thermal conductivity of ZIF-8 were investigated by MD simulations in this work.

2. METHODOLOGY

ZIF-8 is composed of a zinc node and the organic ligand: 2-methylimidiazole in sodalite zeolite-like topology[23] with a space group of $I\bar{4}3m$. A 2 × 2 × 2 supercell of ZIF-8 was used for molecular simulation as shown in Figure 1. The force field of ZIF-8 was adopted from Hu et al.'s study,[24] which has been validated for accurately describing the crystalline, mechanical, and thermophysical properties of ZIF-8. The ZIF-8 framework is flexible throughout MD simulations. Regarding adsorbates, TraPPE force field[25−27] for ethanol and TIP4P/2005 model[28] for water were employed in simulations. The TIP4P/2005 model for water has been validated to exhibit high accuracy in predicting the thermodynamic properties[28] and is in good agreement with experimental measurement of thermal conductivity.[29] The detailed force field parameters have been provided in Tables S1−S4 of the Supporting Information. The initial configurations of ZIF-loaded ethanol/water molecules were obtained from grand canonical Monte Carlo (GCMC) simulation, the MD simulations of ethanol/water loaded in ZIF-8 were taken from the snapshots of equilibrated grand canonical Monte Carlo (GCMC) simulation using RASPA 1.9,[30] in which 2, 4, 6, 8, and 10 ethanol/water molecules were randomly inserted into ZIF-8 with equal probability of rotation and translation. A total of 2 × 10^4 Monte Carlo cycles were implemented, with 1 × 10^4 cycles for equilibration and 1 × 10^4 cycles for production, from which the interaction between ZIF-8 and adsorbates can be obtained.

DOI: 10.1021/acs.jpcc.9b08187
J. Phys. Chem. C 2019, 123, 27369−27374

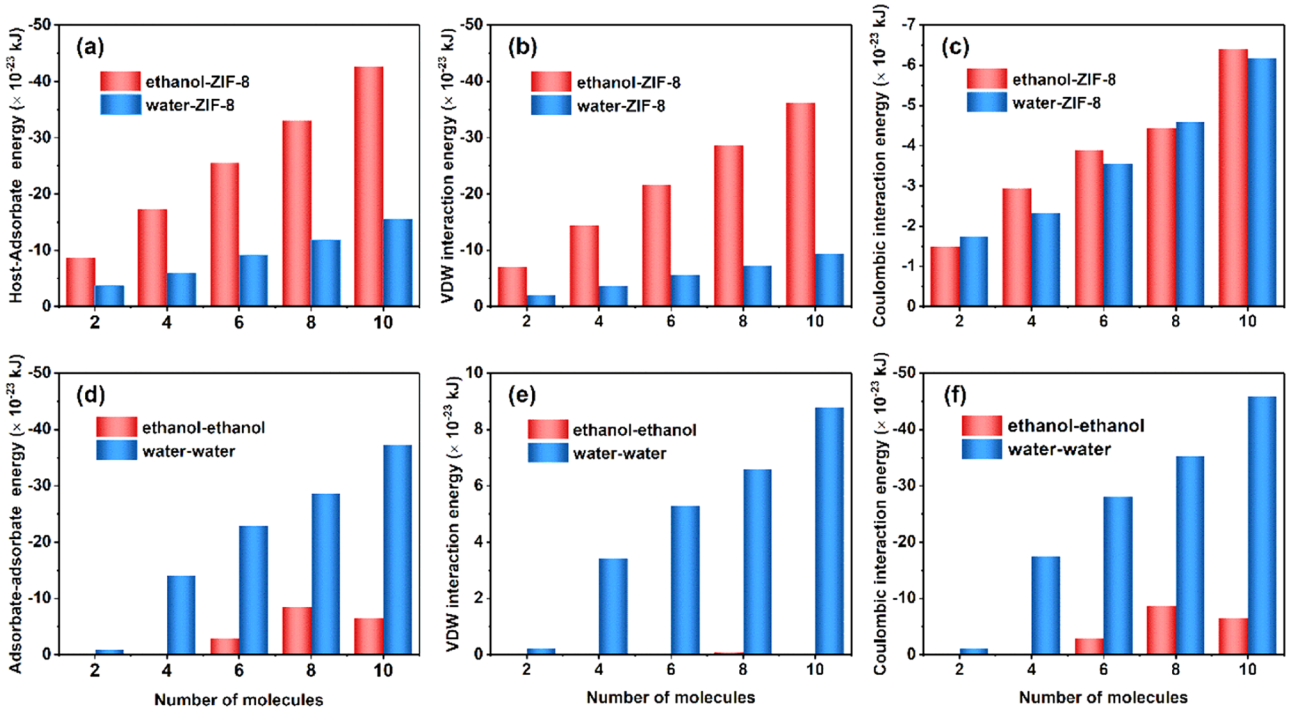

Figure 3. (a) Host−adsorbate and (d) adsorbate−adsorbate interaction energy as well as contributions from (b, e) van der Waals and (c, f) Coulombic interactions.

Equilibrium molecular dynamics simulations are used to calculate the required instantaneous heat flux terms. All simulations was carried out using the large-scale atomic/molecular massively parallel simulator package.[31] The ethanol/water-loaded ZIF-8 was first relaxed at 300 K and 1 bar for 1 ns using the Nosé−Hoover thermostat and barostat.[32,33] Then, MD simulation was performed in NVT (constant number N of particles, volume V and temperature T) ensemble for 2 ns, followed by simulation in NVE (constant number N of particles, volume V and total energy E) ensemble for 1 ns. The time step used in the MD simulation was 1 fs. The Green−Kubo method[34] based on calculating the instantaneous heat flux in an equilibrium MD simulation were applied to predict the thermal conductivity as in eq 1

$$\kappa = \frac{V}{3k_B T^2} \int \langle \vec{J}(0)\cdot\vec{J}(t)\rangle \, dt \tag{1}$$

where V is the volume, k_B is the Boltzmann constant, T is the temperature, $\vec{J}$ is the heat flux, and $\langle\ \rangle$ is the time average.[19] $\langle \vec{J}(0)\cdot\vec{J}(t)\rangle$ can be defined as the heat current autocorrelation function (HCACF).

$$\text{HCACF} = \langle \vec{J}(0)\cdot\vec{J}(t)\rangle \tag{2}$$

To achieve the convergence for the thermal conductivity of ZIF-8 with adsorbed ethanol/water, every successive 10 ps of heat current data was used for estimating the thermal conductivities, which achieves the convergence when HCACF is close to zero.

3. RESULTS AND DISCUSSION

Figure 2a,b shows the thermal conductivity as a function of time, implicating that the thermal conductivity converges slowly and reaches a constant value at about 10 ps. It can be found that the increase in thermal conductivity of ZIF-8 upon ethanol adsorption (Figure 2a) is obviously higher compared with that on water adsorption (Figure 2b). The estimated thermal conductivity of pure ZIF-8 is 0.165 W m^{-1} K^{-1}. Upon adsorption of ethanol/water molecules, the thermal conductivity increases with increased number of adsorbed molecules (Figure 2c). The enhancement is more remarkable for ethanol/ZIF-8, which increases from 0.165 to 0.319 W m^{-1} K^{-1}. On the contrary, no significant increase in water/ZIF-8 is observed (∼0.190 W m^{-1} K^{-1}). At high loading, the thermal conductivity of ZIF-8 was not remarkably changed with the increased number of adsorbed ethanol/water molecules (Figure 2c), which is ∼0.396 W m^{-1} K^{-1} for ethanol/ZIF-8 and ∼0.227 W m^{-1} K^{-1} for water/ZIF-8. In Figure 2d, the ratio between the increment of thermal conductivity ($\Delta\kappa$) relative to the pure ZIF-8 and the total thermal conductivity (κ) can clearly demonstrate the distinct impacts of ethanol and water adsorption on the thermal conductivity of ZIF-8. Such a tendency may be related to the different host−adsorbate interaction between ZIF-8 and ethanol/water, which further imposes effects on the vibration of crystals.

To elucidate the effects of host−adsorbate interaction on the thermal conductivity of ZIF-8 with adsorbed ethanol/water, contributions from both van der Waals and Coulombic interactions for ZIF-8 with adsorbed ethanol/water are presented in Figure 3a−c. Obviously, the stronger interaction between ZIF-8 and ethanol was observed compared to water regardless of the adsorption capacity, which also increased with the increased number of adsorbed molecules. This trend is consistent with their thermal conductivity change, implicating the possible correlation between the host−adsorbate interaction strength and thermal conductivity. Further analysis revealed that the increased host−adsorbate interaction between ZIF-8 and ethanol is mainly contributed by the van der Waals (Figure 3b) instead of Coulombic interaction (Figure 3c). In contrast, the adsorbate−adsorbate interaction (Figure 3d−f) mainly resulting from the Coulombic

DOI: 10.1021/acs.jpcc.9b08187
J. Phys. Chem. C 2019, 123, 27369−27374

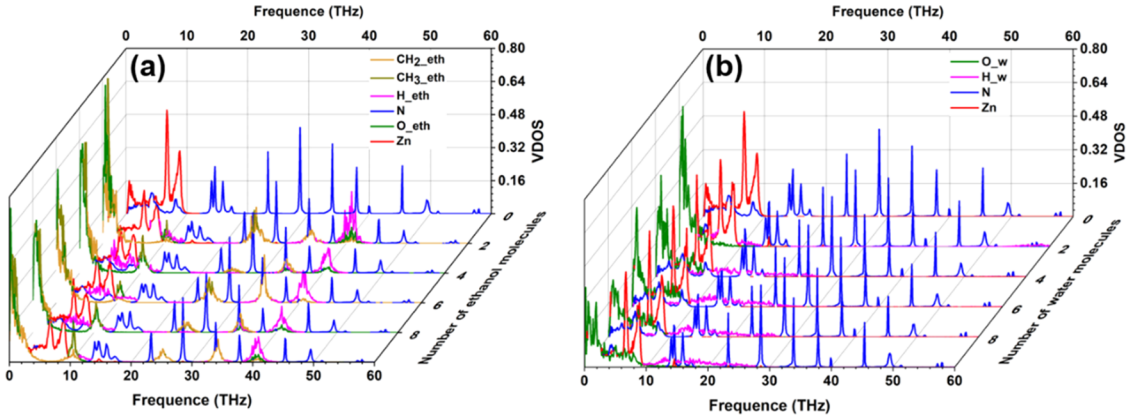

Figure 4. Vibrational density of states (VDOSs) for the framework (Zn and N) and gas (C, O, and H) atoms of ZIF-8 loaded with (a) ethanol and (b) water at 300 K.

interaction seems not to contribute much to the thermal conductivity, which displays the opposite trend to the their thermal conductivity. Besides, ZIF-8/water exhibits a higher adsorbate−adsorbate interaction than ZIF-8/ethanol due to the strong hydrogen network formed in water. However, the interaction of ethanol−ethanol molecules can be negligible. Such results manifest that the influence of the interaction of adsorbate−adsorbate on the thermal conductivity is negligible, whereas the interaction between ZIF-8 and adsorbates plays a dominant role. It can be assumed that the ethanol adsorption may enhance the vibration frequency of ZIF-8 due to their strong interaction, thus leading to a high thermal conductivity.

To demonstrate such a correlation, the vibrational density of states (VDOS) of ZIF-8 with the adsorbed ethanol/water was calculated by taking the Fourier transform of the atomic velocity autocorrelation function (VACF)[35] using the following equation

$$\mathrm{VDOS}(\nu) = \int \gamma(t) \exp(-2\pi i \nu t)\, \mathrm{d}t \tag{3}$$

where ν is the frequency, i is the imaginary unit, and VACF is defined as

$$\gamma(t) = \frac{\langle \sum_i \nu_i(0)\cdot\nu_i(t)\rangle}{\langle \sum_i \nu_i(0)\cdot\nu_i(0)\rangle} \tag{4}$$

Figure 4 shows the VDOS of the framework atoms (i.e., Zn and N), ethanol, and water atoms (i.e., C, O, and H) at 300 K. The VDOSs of Zn, O, and C ($-CH_3$, ethanol) are within 0−10 THz, while the VDOS for N is widely dispersed over 0−60 THz. In addition, the VDOS for C ($-CH_2$, ethanol) is dispersed over 0−40 THz, and the VDOS of H(ethanol) is within 0−10 THz and 38−42 THz in Figure 4a. The overlap between the VDOS of ZIF-8 (Zn and N atoms) and ethanol (CH_2, H, O) atoms suggests the enhanced thermal conductivity. However, the mismatch in the VDOSs of ZIF-8 and water (H and O) atoms is less evident in Figure 4b, implicating the lower thermal conductivity upon water adsorption. The large mismatch between the two VDOSs of Zn and N may cause interfacial phonon scattering, which impedes phonon transport at the solid−solid interface and reduces the thermal conductivity.[19] With the increase of the number of adsorbed molecules, the overlap in the VDOSs of Zn and N of ZIF-8 from 0 to 10 THz is enhanced.

We further calculated the overlapped energy (E_{overlap}) between Zn and N atoms as a function of the number of molecules in Figure 5.

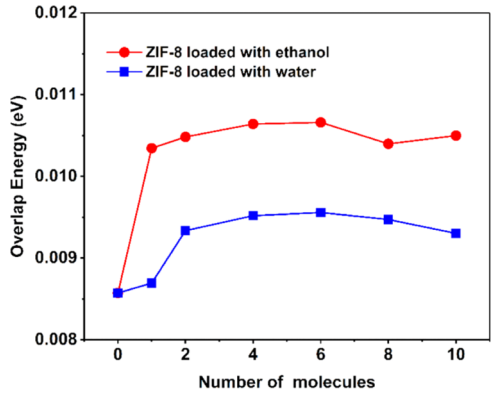

Figure 5. Overlapped energy between Zn and N atoms as a function of the number of molecules of ethanol and water.

The overlap energy[19] was estimated by

$$E_{\mathrm{overlap}} = \int g_o(\nu) \frac{h\nu}{\exp(h\nu/k_B T) - 1} \mathrm{d}\nu \tag{5}$$

where E_{overlap} is the phonon energy in the overlap region $g_o(\nu)$, h is the Planck constant, ν is the phonon frequency, and $1/(\exp(h\nu/k_B T) - 1)$ is the Bose−Einstein distribution.

With the number of adsorbed molecules increasing from 0 to 10, the overlap energy is significantly increased and then stayed nearly constant, implicating that the gas adsorption imposed remarkable impacts on the VDOSs of Zn and N atoms, in turn leading to the enhanced thermal conductivity of the system. The high overlap energy indicated the high probability of phonon−gas molecule collisions with the increased number of adsorbed gas molecules, thus probably leading to high thermal conductivity. It should be noted that the thermal conductivity of the system is the combined effects of each atom in the system rather than simply determined by the E_{overlap} between Zn and N. Furthermore, the higher overlap energy of ZIF-8/ethanol than that of ZIF-8/water is possibly ascribed to the stronger interaction between ethanol and ZIF-8, leading to the better heat transfer in ZIF-8/ethanol.

DOI: 10.1021/acs.jpcc.9b08187
J. Phys. Chem. C 2019, 123, 27369−27374

4. CONCLUSIONS

In this work, we investigated the effects of ethanol/water adsorption on the thermal conductivity of ZIF-8 by molecular dynamics simulations. It was found that the predicted thermal conductivity of ZIF-8 upon ethanol adsorption is higher than that upon water adsorption, which also increases with the number of adsorbed ethanol molecules. Such a trend correlates with the interaction energy between ZIF-8 and adsorbed gas molecules, i.e., the stronger interaction between ZIF-8 and ethanol gives rise to higher thermal conductivity than the ZIF-8/water systems. The VDOS analysis demonstrated the increased overlap between VDOS of Zn and N atoms with the increased number of adsorbed ethanol molecules, thus leading to the enhanced overlap energy that is favorable for heat transfer. It should be noted that the findings from this work may vary depending on the type of MOFs and adsorbates. Although further experimental investigation is required to validate these findings, it is currently a challenging task due to the limitation of the direct measurement of thermal conductivity of single MOF crystal with adsorbed gas molecules. Besides, understanding the heat transfer mechanism from molecular perspective may provide helpful insights into the development of new techniques to enhance heat transfer in nanoporous materials by choosing the proper adsorbents and adsorbates.

■ ASSOCIATED CONTENT

Supporting Information

The Supporting Information is available free of charge on the ACS Publications website at DOI: 10.1021/acs.jpcc.9b08187.

Detailed force field parameters of ZIF-8, water, and ethanol, and the effects of different water models on the thermal conductivity and interaction of ZIF-8 (PDF)

■ AUTHOR INFORMATION

Corresponding Authors

*E-mail: hypeng@hust.edu.cn. (H.P.).
*E-mail: songli@hust.edu.cn. (S.L.).

ORCID

Wei Li: 0000-0002-3920-3863
Haiyan Peng: 0000-0002-0083-8589
Song Li: 0000-0003-3552-3250

Notes

The authors declare no competing financial interest.

■ ACKNOWLEDGMENTS

This work was funded by the National Natural Science Foundation of China (NSFC) under Project No. 51606081 and Hubei Provincial Nature Science Foundation (No. 2019CFB456). This work was also supported by the double first-class research funding of China-EU Institute for Clean and Renewable Energy (No. ICARE-RP-2018-HYDRO-001) and the Graduates' Innovation Fund of Huazhong University of Science and Technology (No. 2019YGSCXCY026).

■ REFERENCES

(1) Li, H.; Wang, K.; Sun, Y.; Lollar, C. T.; Li, J.; Zhou, H.-C. Recent Advances in Gas Storage and Separation Using Metal–Organic Frameworks. *Mater. Today* **2018**, *21*, 108–121.

(2) Kunowsky, M.; Marco-Lózar, J. P.; Linares-Solano, A. Material Demands for Storage Technologies in a Hydrogen Economy. *J. Renewable Energy* **2013**, *2013*, No. 878329.

(3) Petit, C. Present and Future of MOF Research in the Field of Adsorption and Molecular Separation. *Curr. Opin. Chem. Eng.* **2018**, *20*, 132–142.

(4) Dolgopolova, E. A.; Rice, A. M.; Martin, C. R.; Shustova, N. B. Photochemistry and Photophysics of MOFs: Steps Towards MOF-Based Sensing Enhancements. *Chem. Soc. Rev.* **2018**, *47*, 4710–4728.

(5) Zhang, M.; Dai, Q.; Zheng, H.; Chen, M.; Dai, L. Novel MOF-Derived Co@N-C Bifunctional Catalysts for Highly Efficient Zn-Air Batteries and Water Splitting. *Adv. Mater.* **2018**, *30*, No. 1705431.

(6) Kim, H.; Yang, S.; Rao, S. R.; Narayanan, S.; Kapustin, E. A.; Furukawa, H.; Umans, A. S.; Yaghi, O. M.; Wang, E. N. Water Harvesting from Air with Metal-Organic Frameworks Powered by Natural Sunlight. *Science* **2017**, *356*, 430–434.

(7) Li, B.; Wen, H. M.; Zhou, W.; Chen, B. Porous Metal-Organic Frameworks for Gas Storage and Separation: What, How, and Why? *J. Phys. Chem. Lett.* **2014**, *5*, 3468–3479.

(8) Ma, S.; Sun, D.; Simmons, J. M.; Collier, C. D.; Yuan, D.; Zhou, H.-C. Metal-Organic Framework from an Anthracene Derivative Containing Nanoscopic Cages Exhibiting High Methane Uptake. *J. Am. Chem. Soc.* **2008**, *130*, 1012–1016.

(9) Song, X. Z.; Song, S. Y.; Zhu, M.; Hao, Z. M.; Meng, X.; Zhao, S. N.; Zhang, H. J. Employing Tripodal Carboxylate Ligand to Construct Co(II) Coordination Networks Modulated by N-Donor Ligands: Syntheses, Structures and Magnetic Properties. *Dalton Trans.* **2013**, *42*, 13231–13240.

(10) Makal, T. A.; Li, J. R.; Lu, W.; Zhou, H. C. Methane Storage in Advanced Porous Materials. *Chem. Soc. Rev.* **2012**, *41*, 7761–7779.

(11) de Lange, M. F.; Verouden, K. J.; Vlugt, T. J.; Gascon, J.; Kapteijn, F. Adsorption-Driven Heat Pumps: The Potential of Metal-Organic Frameworks. *Chem. Rev.* **2015**, *115*, 12205–12250.

(12) Han, L.; Budge, M.; Alex Greaney, P. Relationship between Thermal Conductivity and Framework Architecture in MOF-5. *Comput. Mater. Sci.* **2014**, *94*, 292–297.

(13) Babaei, H.; Wilmer, C. E. Mechanisms of Heat Transfer in Porous Crystals Containing Adsorbed Gases: Applications to Metal-Organic Frameworks. *Phys. Rev. Lett.* **2016**, *116*, No. 025902.

(14) Babaei, H.; McGaughey, A. J. H.; Wilmer, C. E. Effect of Pore Size and Shape on the Thermal Conductivity of Metal-Organic Frameworks. *Chem. Sci.* **2017**, *8*, 583–589.

(15) Cui, B.; Audu, C. O.; Liao, Y.; Nguyen, S. T.; Farha, O. K.; Hupp, J. T.; Grayson, M. Thermal Conductivity of ZIF-8 Thin-Film under Ambient Gas Pressure. *ACS Appl. Mater. Interfaces* **2017**, *9*, 28139–28143.

(16) Gunatilleke, W.; Wei, K.; Niu, Z.; Wojtas, L.; Nolas, G.; Ma, S. Thermal Conductivity of a Perovskite-Type Metal-Organic Framework Crystal. *Dalton Trans.* **2017**, *46*, 13342–13344.

(17) Huang, B. L.; Ni, Z.; Millward, A.; McGaughey, A. J. H.; Uher, C.; Kaviany, M.; Yaghi, O. Thermal Conductivity of a Metal-Organic Framework (MOF-5): Part II. Measurement. *Int. J. Heat Mass Transfer* **2007**, *50*, 405–411.

(18) Huang, B. L.; McGaughey, A. J. H.; Kaviany, M. Thermal Conductivity of Metal-Organic Framework 5 (MOF-5): Part I. Molecular Dynamics Simulations. *Int. J. Heat Mass Transfer* **2007**, *50*, 393–404.

(19) Zhang, X.; Jiang, J. Thermal Conductivity of Zeolitic Imidazolate Framework-8: A Molecular Simulation Study. *J. Phys. Chem. C* **2013**, *117*, 18441–18447.

(20) Huang, J.; Xia, X.; Hu, X.; Li, S.; Liu, K. A General Method for Measuring the Thermal Conductivity of MOF Crystals. *Int. J. Heat Mass Transfer* **2019**, *138*, 11–16.

(21) Zhang, K.; Lively, R. P.; Dose, M. E.; Brown, A. J.; Zhang, C.; Chung, J.; Nair, S.; Koros, W. J.; Chance, R. R. Alcohol and Water Adsorption in Zeolitic Imidazolate Frameworks. *Chem. Commun.* **2013**, *49*, 3245–3247.

(22) Zhang, K.; Lively, R. P.; Zhang, C.; Chance, R. R.; Koros, W. J.; Sholl, D. S.; Nair, S. Exploring the Framework Hydrophobicity and

DOI: 10.1021/acs.jpcc.9b08187
J. Phys. Chem. C 2019, 123, 27369–27374

Flexibility of ZIF-8: From Biofuel Recovery to Hydrocarbon Separations. *J. Phys. Chem. Lett.* **2013**, *4*, 3618−3622.
(23) Ortiz, A. U.; Freitas, A. P.; Boutin, A.; Fuchs, A. H.; Coudert, F. X. What Makes Zeolitic Imidazolate Frameworks Hydrophobic or Hydrophilic? The Impact of Geometry and Functionalization on Water Adsorption. *Phys. Chem. Chem. Phys.* **2014**, *16*, 9940−9949.
(24) Hu, Z.; Zhang, L.; Jiang, J. Development of a Force Field for Zeolitic Imidazolate Framework-8 with Structural Flexibility. *J. Chem. Phys.* **2012**, *136*, No. 244703.
(25) Chen, B.; Potoff, J. J.; Siepmann, J. I. Monte Carlo Calculations for Alcohols and Their Mixtures with Alkanes. Transferable Potentials for Phase Equilibria. 5. United-Atom Description of Primary, Secondary, and Tertiary Alcohols. *J. Phys. Chem. B* **2001**, *105*, 3093−3104.
(26) Jorgensen, W. L. Optimized Intermolecular Potential Functions for Liquid Alcohols. *J. Phys. Chem. A.* **1986**, *90*, 1276−1284.
(27) Martin, M. G.; Siepmann, J. I. Transferable Potentials for Phase Equilibria. 1. United-Atom Description of n-Alkanes. *J. Phys. Chem. B* **1998**, *102*, 2569−2577.
(28) Abascal, J. L.; Vega, C. A General Purpose Model for the Condensed Phases of Water: TIP4P/2005. *J. Chem. Phys.* **2005**, *123*, No. 234505.
(29) Römer, F.; Lervik, A.; Bresme, F. Nonequilibrium Molecular Dynamics Simulations of the Thermal Conductivity of Water: A Systematic Investigation of the SPC/E and TIP4P/2005 Models. *J. Chem. Phys.* **2012**, *137*, No. 074503.
(30) Dubbeldam, D.; Calero, S.; Ellis, D. E.; Snurr, R. Q. RASPA: Molecular Simulation Software for Adsorption and Diffusion in Flexible Nanoporous Materials. *Mol. Simul.* **2016**, *42*, 81−101.
(31) Plimpton, S. J. Fast Parallel Algorithms for Short-Range Molecular Dynamics. *J. Comput. Phys.* **1995**, *117*, 1−19.
(32) Nosé, S. A Unified Formulation of the Constant Temperature Molecular Dynamics Methods. *J. Chem. Phys.* **1984**, *81*, 511−519.
(33) Hoover, W. G. Canonical Dynamics: Equilibrium Phase-Space Distributions. *Phys. Rev. A* **1985**, *31*, 1695−1697.
(34) Schelling, P. K.; Phillpot, S. R.; Keblinski, P. Comparison of Atomic-Level Simulation Methods for Computing Thermal Conductivity. *Phys. Rev. B* **2002**, *65*, No. 144306.
(35) Dickey, J. M.; Paskin, A. Computer Simulation of the Lattice Dynamics of Solids. *Phys. Rev.* **1969**, *188*, 1407−1418.

DOI: 10.1021/acs.jpcc.9b08187
J. Phys. Chem. C 2019, 123, 27369−27374